Stabilization of heterogeneous silicon lasers using Pound-Drever-Hall locking to Si_3N_4 ring resonators

Daryl T. Spencer,[1,*] Michael L. Davenport,[1] Tin Komljenovic,[1] Sudharsanan Srinivasan,[1,2] and John E. Bowers[1]

[1]*University of California Santa Barbara, Santa Barbara, CA, 93106, USA*
[2]*Aurrion Inc., Goleta, CA, 93117, USA*
**darylt@ece.ucsb.edu*

Abstract: Recent results on heterogeneous Si/III-V lasers and ultra-high Q Si_3N_4 resonators are implemented in a Pound-Drever-Hall frequency stabilization system to yield narrow linewidth characteristics for a stable on-chip laser reference. The high frequency filtering is performed with Si resonant mirrors in the laser cavity. To suppress close in noise and frequency walk off, the laser is locked to an ultra-high Q Si_3N_4 resonator with a 30 million quality factor. The laser shows high frequency noise levels of 60×10^3 Hz^2/Hz corresponding to 160 kHz linewidth, and the low frequency noise is suppressed 33 dB to 10^3 Hz^2/Hz with the PDH system.

OCIS codes: (140.3425) Laser stabilization; (130.0130) Integrated optics; (140.4780) Optical resonators.

References and links

1. T. J. Kippenberg, R. Holzwarth, and S. A. Diddams, "Microresonator-based optical frequency combs," Science **332**(6029), 555–559 (2011).
2. P. Del'Haye, O. Arcizet, A. Schliesser, R. Holzwarth, and T. J. Kippenberg, "Full Stabilization of a Microresonator-Based Optical Frequency Comb," Phys. Rev. Lett. **101**(5), 053903 (2008).
3. S. B. Papp, K. Beha, P. Del'Haye, F. Quinlan, H. Lee, K. J. Vahala, and S. A. Diddams, "Microresonator frequency comb optical clock," Optica **1**(1), 10 (2014).
4. J. Li, S. Diddams, and K. J. Vahala, "Pump frequency noise coupling into a microcavity by thermo-optic locking," Opt. Express **22**(12), 14559–14567 (2014).
5. A. J. Seeds and K. J. Williams, "Microwave Photonics," J. Lightwave Technol. **24**(12), 4628–4641 (2006).
6. L. A. Coldren, S. C. Nicholes, L. Johansson, S. Ristic, R. S. Guzzon, E. J. Norberg, and U. Krishnamachari, "High Performance InP-Based Photonic ICs—A Tutorial," J. Lightwave Technol. **29**(4), 554–570 (2011).
7. J.-F. Cliche, Y. Painchaud, C. Latrasse, M.-J. Picard, I. Alexandre, and M. Têtu, "Ultra-Narrow Bragg Grating for Active Semiconductor Laser Linewidth Reduction through Electrical Feedback," in *Bragg Gratings, Photosensitivity, and Poling in Glass Waveguides* (2007), p. BTuE2.
8. A. Sivananthan, H. Park, M. Lu, J. S. Parker, E. Bloch, L. A. Johansson, M. J. Rodwell, and L. A. Coldren, "Monolithic Linewidth Narrowing of a Tunable SG-DBR Laser," in *Optical Fiber Communication Conference/National Fiber Optic Engineers Conference 2013* (OSA, 2013), p. OTh3I.3.
9. E. D. Black, "An introduction to Pound–Drever–Hall laser frequency stabilization," Am. J. Phys. **69**(1), 79–87 (2001).
10. W. Zhang, M. J. Martin, C. Benko, J. L. Hall, J. Ye, C. Hagemann, T. Legero, U. Sterr, F. Riehle, G. D. Cole, and M. Aspelmeyer, "Reduction of residual amplitude modulation to 1×10^{-6} for frequency modulation and laser stabilization," Opt. Lett. **39**(7), 1980–1983 (2014).
11. D. T. Spencer, J. F. Bauters, M. J. R. Heck, and J. E. Bowers, "Integrated waveguide coupled Si_3N_4 resonators in the ultrahigh-Q regime," Optica **1**(3), 153–157 (2014).
12. S. Srinivasan, M. Davenport, T. Komljenovic, J. Hulme, D. T. Spencer, and J. E. Bowers, "Coupled-Ring-Resonator-Mirror-Based Heterogeneous III–V Silicon Tunable Laser," IEEE Photonics J. **7**(3), 2700908 (2015).
13. N. M. Sampas, "A ring laser gyroscope with optical subtraction," (1990), Chap. II.5.
14. D. Derickson, *Fiber Optic Test and Measurement* (Prentice Hall, 1998), Chap. 5.
15. J. F. Bauters, M. J. R. Heck, D. D. John, J. S. Barton, C. M. Bruinink, A. Leinse, R. G. Heideman, D. J. Blumenthal, and J. E. Bowers, "Planar waveguides with less than 0.1 dB/m propagation loss fabricated with wafer bonding," Opt. Express **19**(24), 24090–24101 (2011).
16. R. Fox, C. Oates, and L. Hollberg, "Stabilizing diode lasers to high-finesse cavities," in *Experimental Methods in the Physical Sciences: Cavity-Enhanced Spectroscopies*, R. D. van Zee and J. P. Looney, eds. (Academic Press, 2003).

#259801 Received 22 Feb 2016; revised 6 Apr 2016; accepted 6 Apr 2016; published 9 Jun 2016

17. H. Lee, M.-G. Suh, T. Chen, J. Li, S. A. Diddams, and K. J. Vahala, "Spiral resonators for on-chip laser frequency stabilization," Nat. Commun. **4**, 2468 (2013).
18. M. J. R. Heck, J. F. Bauters, M. L. Davenport, D. T. Spencer, and J. E. Bowers, "Ultra-low loss waveguide platform and its integration with silicon photonics," Laser Photonics Rev. **8**(5), 667–686 (2014).
19. M. Ohtsu, "Structure and Oscillation Mechanisms," in *Highly Coherent Semiconductor Lasers* (Artech House, 1992).
20. L. Chen, A. Sohdi, J. E. Bowers, L. Theogarajan, J. Roth, and G. Fish, "Electronic and photonic integrated circuits for fast data center optical circuit switches," IEEE Commun. Mag. **51**(9), 53–59 (2013).

1. Introduction

Future integrated laser systems for metrology, stabilization, and other high signal-to-noise (S/N) ratio applications demand lower linewidths and their related frequency noise (FM) power spectral density (PSD). One example is pump lasers for optical frequency combs [1], which require a controllable and highly stable laser frequency since the pump's noise is transferred to the comb, and subsequent precise timing reference [2–4]. The integration of such a system requires an efficient comb generator, but also a high power laser with a very high quality factor (Q) resonator as its reference. With a stable reference laser as an integrated local oscillator (LO), optical phase locked loops and other coherent demodulation schemes can become higher performance, more compact, and consume less power with closely integrated drivers and controllers [5,6].

Many wavelength locking systems on chip scale platforms utilize sideband, or "fringe", locking where the laser is positioned on an amplitude slope of an interferometer or resonator [7,8]. However, fringe locking has issues with S/N, AM versus FM discrimination, and low frequency flicker noise in the generation of the error signal at baseband. The most stable laser locking systems to date utilize the Pound-Drever-Hall (PDH) system [9], which reduces the frequency noise of a tunable laser via an RF lock to a reference resonator. With PDH modulation, the resonator is required to have a very high Q, and has typically been free space coupled with ultra-low expansion glass and placed in a vacuum chamber for thermal stability [10]. In this paper, we will bridge this gap by utilizing waveguide coupled ultra-high (30 million) Q resonators that can sustain PDH locking [11], and narrow (160 kHz Lorentzian) linewidth heterogeneous Si/III-V lasers that can be integrated on a single chip [12]. We will then show a system demonstration of the noise suppression capability using these integrable devices, yielding up to 33 dB reduction in FM PSD at a few kHz offset frequencies. This result can be extended to realize a fully integrated stable narrow linewidth laser source on a single chip which can provide large improvements in consumed power and cost.

2. The PDH system & components

The PDH system is a laser frequency stabilization scheme that requires RF phase modulation of a tunable laser beyond the full width half maximum (FWHM) of the reference high Q resonator. The resonator acts as a frequency discriminator and performs the FM to AM conversion, more efficiently in the through port (notch filter) configuration due to higher carrier suppression and sideband recovery outside the bandwidth than the drop port [13]. The optical signal is then detected on a high speed photodetector (PD) and transimpedance amplifier (TIA). This RF signal is demodulated on a mixer with the same signal generator driving the laser modulation. The baseband error signal contains information on the difference between the laser frequency and resonance frequency from DC to the modulation frequency. This error signal is then filtered with op-amps and drives the DC portion of the laser's current injection pads in negative feedback. The system schematic is shown in Fig. 1 and the components will be discussed next.

#259801 Received 22 Feb 2016; revised 6 Apr 2016; accepted 6 Apr 2016; published 9 Jun 2016

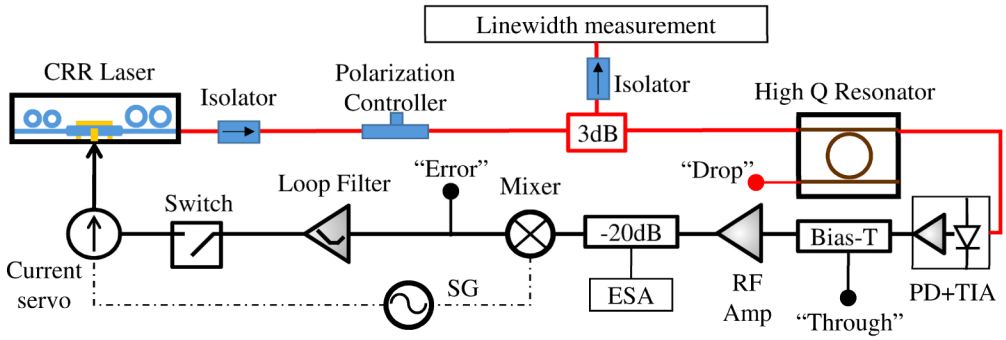

Fig. 1. Schematic of the PDH setup. The coupled ring resonator (CRR) laser is isolated from any spurious reflections and the resonator is packaged with cleaved fiber. Optical fibers are shown in red, with electronic signals shown in black. The black and red bubbles denote monitor points in the system.

2.1 The heterogeneous Si/III-V CRR laser

The laser has 7 × InGaAs/InGaAlAs quantum well gain material heterogeneously integrated with Si waveguide based coupled ring resonator (CRR) mirrors via wafer bonding [12]. Each mirror contains 2 resonators that are appropriately coupled and fabricated with micro-heaters to produce a high Q tunable Vernier in conjunction with the opposite mirror. The lasing wavelength for this study was 1577 nm, and the linewidth was 160 kHz measured via the self-heterodyne method. The current bias, RF frequency drive, and feedback signal are combined in a Vescent D2-105 current servo and probed to the CRR chip on a TEC stage. The laser's output is coupled with a 2 μm spot size lensed fiber, and spliced to an inline fiber isolator and polarization controller to control the polarization launched into the ring resonator. The laser's FM modulation frequency characteristics are measured by low frequency locking a 10 cm unbalanced Mach-Zehnder interferometer (MZI) at quadrature, while performing a network analyzer test [14] with a SRS 770 (500 Hz – 100 kHz) and HP 4396B (100 kHz – 20 MHz), shown in Fig. 2. The laser shows a single pole role off at 70 kHz and resonant peaking at 7.6 MHz. The electrical response of the Vescent servo is also shown in Fig. 2, with a DC response of 1 mA/V and usable bandwidth of 1 MHz before additional phase lag is added.

#259801 Received 22 Feb 2016; revised 6 Apr 2016; accepted 6 Apr 2016; published 9 Jun 2016

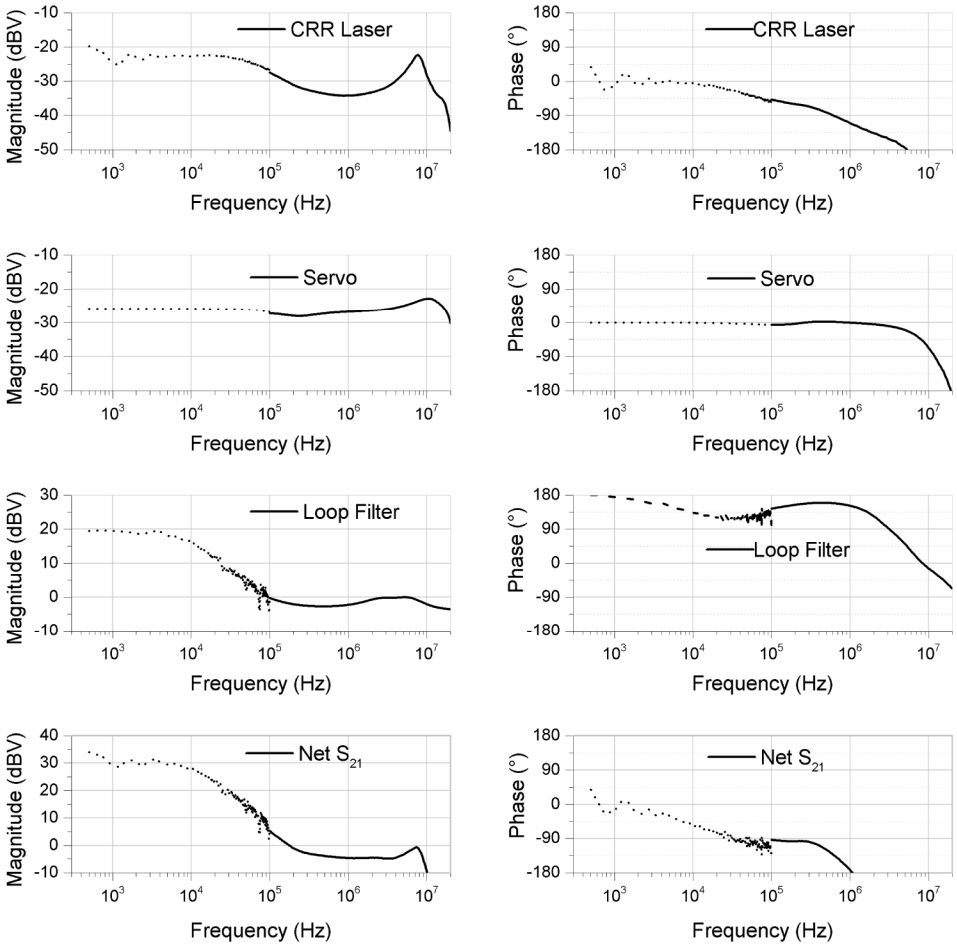

Fig. 2. Bode plots of the CRR laser FM tuning, Vescent servo supply, loop filter electronics, and total transfer function of the feedback loop used in this study. Dotted lines correspond to measurements using a SRS 770 (500 Hz – 100 kHz), and solid lines using a HP 4396B (100 kHz – 20 MHz).

2.2 The ultra-high Q Si_3N_4 resonator

The resonator is based on the ultra-low loss waveguide (ULLW) Si_3N_4 platform, which has demonstrated 0.045 dB/m propagation loss [15] and 81 million unloaded Q factor multimode resonators [11]. In this study, we use a bend radius of 9.8 mm and core thickness of 40 nm Si_3N_4 with bonded thermal SiO_2 cladding and high temperature anneal, but stay in the single mode regime with a waveguide width of 7 μm for system simplicity. This yields a loaded Q factor of 30 million and extinction ratio of 3.5 dB at the operating wavelength of 1577 nm. The resonator has been packaged in an Al case with cleaved fiber, transparent epoxy, and a TEC for slow macro alignment.

2.3 Electronic demodulation and filtered feedback

The PDH electronics are implemented with commercial components in close proximity to the other components to reduce phase lag due to excess delay. The PD + TIA is an Agilent 11982A with 15 GHz bandwidth, and a bias-T is used to monitor the through port DC signal. A broadband RF amplifier increases the RF signal before reaching a –20 dB monitor tap and ZAD-1 + double balanced mixer. The loop filter is implemented with OP27 and AD797 op-

#259801 Received 22 Feb 2016; revised 6 Apr 2016; accepted 6 Apr 2016; published 9 Jun 2016

amps that are soldered onto evaluation boards. A maximum driving capacitance of 1 nF is used to place a low frequency integrator pole at 8 kHz, and a differential gain for compensating the laser roll off is placed at 70 kHz. The frequency response of the loop filter is shown in Fig. 2, and a good reference for design is given in [16].

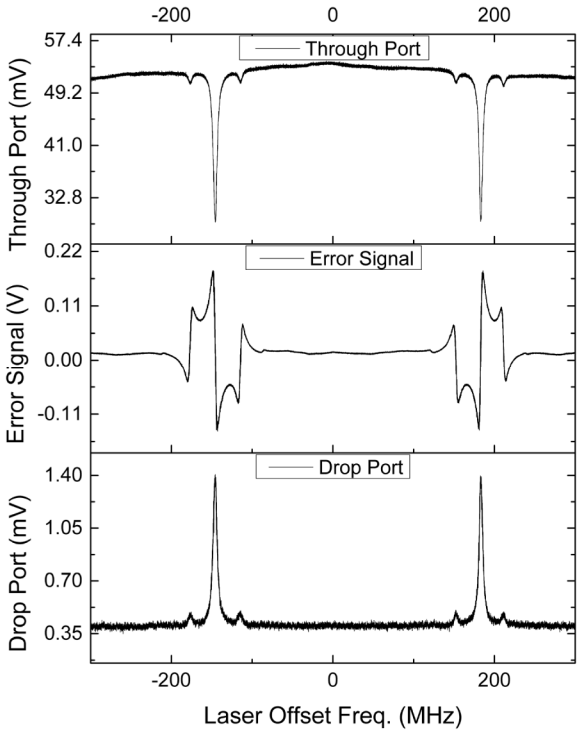

Fig. 3. Open loop calibration of the through port, error signal, and drop port with a ramp signal applied to the laser servo.

3. PDH system results

The open loop response of the system is measured by removing the loop filter, applying a 25 Hz, 3 Vpp ramp and a 30 MHz RF sinusoid to the laser servo, and monitoring the 3 labeled points shown in Fig. 1 on an oscilloscope. The results are shown in Fig. 3, where the through port is monitored via a bias-T, the error signal is taken through an in-line electrical splitter after the mixer, and the drop port is measured on a Thorlabs DET 01CFC photodetector. Using the 30 MHz sidebands as the reference, the laser FM efficiency is 201 MHz/V, and the error signal slope is 86 mV/MHz, yielding a transfer function of 17 V/V near DC. With the DC response and frequency characteristics of the loop, we then lock the laser to the resonance wavelength by connecting the loop filter electronics.

To properly characterize the system performance, we utilize two signals in the PDH system. The first is an absolute measurement on the laser's FM PSD by taking a 3 dB optical tap after the laser output to an isolator, 13 m unbalanced fiber based MZI and PD + TIA. The interferometer contains a fiber stretcher in one arm, and the PD has a monitor tap, which we use to apply a low frequency quadrature or peak locking circuit to measure the FM and AM response, respectively. Once the MZI is locked, the PD + TIA output put goes through a DC block (2 Hz - 40 MHz) and the noise PSD is measured across different spans of a Rhode and Schwarz FSU spectrum analyzer with RMS filters and corrected to the appropriate units of Hz^2/Hz. The RF loss and calibrated transfer function of the MZI are subtracted from the result to yield the laser's FM PSD [14].

#259801 Received 22 Feb 2016; revised 6 Apr 2016; accepted 6 Apr 2016; published 9 Jun 2016

The unlocked laser's high frequency FM PSD (S_v) is measured to be 60 × 10^3 Hz^2/Hz, which aligns perfectly with the previously measured 160 kHz linewidth (Δν) by self-heterodyne method ($\Delta\nu = \pi S_v$ for Lorentzian lineshapes) [12]. This high frequency noise is ≈15 × better than conventional InP DFB lasers, however, at low frequency, there is considerable walk off and the PSD increases as $1/\sqrt{f}$ yielding an unstable laser at microsecond and greater time scales. The locked PDH system suppresses this noise considerably beginning at 200 kHz, and reduces the noise to 10^3 Hz^2/Hz at 3 kHz offset frequency, a reduction of 33 dB compared to the unlocked laser (see Fig. 4). A common phase bump is seen at 1 MHz, and effects of the laser's FM response appear near 4 MHz. The measured AM noise shows that further FM noise reduction is limited by this floor, since the laser servo is unable to further distinguish laser FM noise from AM system noise. We will investigate this noise limit in the next paragraph. Our results compare well to recent PDH results using a commercial external cavity laser, 1.2 m spiral wedge waveguide resonators, and tapered fiber coupling [17], where similar loop bandwidths near 100 kHz and 26 dB of suppression was achieved. By starting with a high power laser with lower high frequency noise, the fully integrated linewidth was reduced, yielding a minimum FM PSD near 3 Hz^2/Hz at 5 kHz offset frequency.

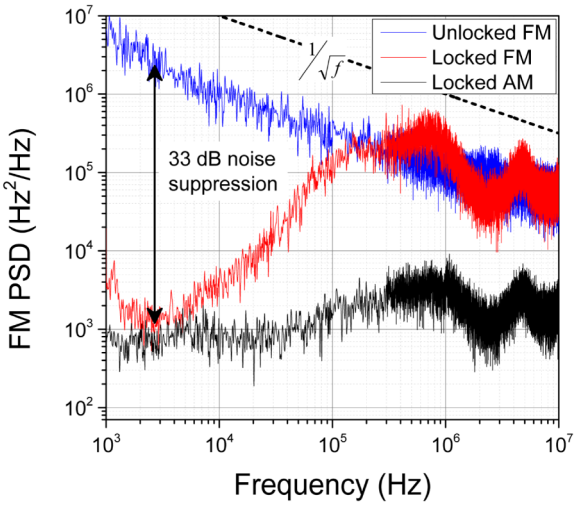

Fig. 4. PSD of the PDH system measured through an unbalanced MZI. At quadrature, the unlocked (blue) and locked (red) FM PSD is given, while the locked AM PSD (black) is measured at the peak of the MZI.

The second measurement used to characterize the system is the 30 MHz RF signal in the feedback circuit. Since this is made inside the feedback loop, the exact noise levels are only good for relative comparison, not absolute measurement. The effect of the locked feedback circuit on the laser's FM noise is written onto the 30 MHz signal, and shows the same phase bump near 1 MHz, and reduction at frequencies less than 200 kHz. The limit of this reduction is found by measuring the shot noise plus laser relative intensity noise (RIN) floor, which is obtained by bypassing the resonator and matching the photocurrent level of the locked system, in this case the dip of the through port. The thermal noise floor is measured with the laser off and amplifiers on, and found to be >8 dB below the shot noise plus RIN floor. The minimum locked noise level is found to be within a few dB of system noise floor, as shown in Fig. 5.

Improvements to the loop could be made with more efficient chip-to-fiber coupling or monolithic waveguide-to-waveguide coupling [18]. This could yield a lower shot noise floor by an estimated 15 dB (9 dB facet loss versus 1.6 dB monolithic), where we would then be

#259801 Received 22 Feb 2016; revised 6 Apr 2016; accepted 6 Apr 2016; published 9 Jun 2016

limited by thermal noise. This could then be reduced by increasing the quality factor of the resonator, which increases the error signal slope, and thus less electrical amplification is needed. Additionally, the CRR laser cavity yields a nonlinear FM tuning response beyond the loop bandwidth of 200 kHz, most likely due to the combination of thermal and carrier plasma effects [19]. Programmable digital loop filters can design for these nonlinear effects and closer monolithic or system-in-package integration of the full optoelectronic loop [8,18,20] will keep the phase lag due to loop delay low.

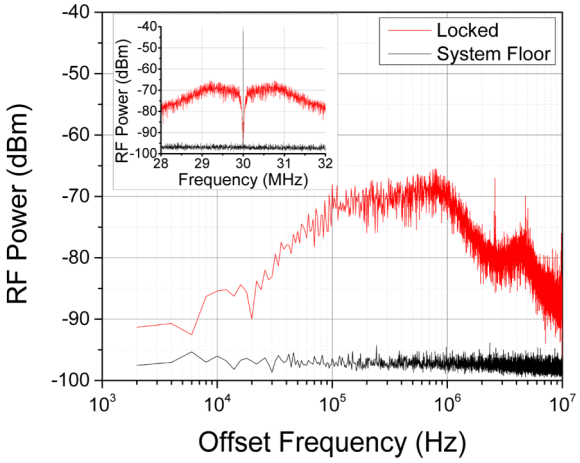

Fig. 5. In-loop characterization of the 30 MHz RF signal in linear (inset) and log scale.

4. Conclusion

We have successfully demonstrated a PDH frequency stabilization system using a heterogeneous Si CRR laser, waveguide coupled Si_3N_4 resonator, and appropriate feedback electronics. The high frequency FM noise is measured to be 60×10^3 Hz^2/Hz consistent with a 160 kHz linewidth. Within the loop bandwidth of the PDH lock, the low frequency noise is suppressed up to 33 dB, to 10^3 Hz^2/Hz. The ultra-high Q Si_3N_4 cavity allows for 60 × reduction of noise below the spontaneous emission noise of the laser, making it very promising for further integration work. Lower coupling losses on a monolithic platform will improve the system performance, and electronics in closer proximity to the devices will allow for higher loop bandwidths and noise suppression.

Acknowledgments

This research was supported by the DARPA EPHI program. The authors thank Luke Theogarajan and Aaron Bluestone for helpful discussions.

#259801 Received 22 Feb 2016; revised 6 Apr 2016; accepted 6 Apr 2016; published 9 Jun 2016